DETECTOR CHARACTERIZATION OF ADVANCED LIGO

By

Thomas J. Massinger

B.S. Physics, Utica College, Utica, NY 13502

DISSERTATION
SUBMITTED IN PARTIAL FULFILLMENT OF THE REQUIREMENTS
FOR THE DEGREE OF
DOCTOR OF PHILOSOPHY IN PHYSICS

Syracuse University
August 2016

Approved : _____

Prof. Peter R. Saulson

Date : _____

ABSTRACT

Placeholder with test reference ([1]).

ACKNOWLEDGEMENTS

I need to thank a whole lot of people.

Contents

List of Tables

List of Figures

Preface

The work presented in this thesis stems from my participation in the LIGO Scientific Collaboration (LSC). This work does not reflect the scientific opinion of the LSC and it was not reviewed by the collaboration.

Well that was fun.

Chapter 1

Introduction

Write down some basics

1.1 The Advanced LIGO Interferometers

1.2 Searching for Compact Binary Coalescences

1.3 Detector Characterization

Chapter 2

Instrumental Detector Characterization

2.1 Description of instrumental DetChar

I did a whole lot of instrumental DetChar.

2.2 Tools and algorithms

2.2.1 Omicron

We use a sine-Gaussian basis to search for excess power

2.2.2 Hveto

Time correlations are used to search for auxiliary channels with glitches that correlate with DARM.

2.3 Analog-to-Digital Conversion

Advanced LIGO interferometers are controlled in real-time using a digital control system installed on a series of computers referred to as front end computers. This system overall is referred to as the Front End Control (FEC) subsection of the more expansive Control and Data System (CDS). In a control loop, the FE computers must be capable of reading in an analog signal from the interferometer (position

measurements, error signals, coil currents, etc), digitally sampling that analog signal, using these now digital values in a series of control algorithms, and outputting an analog control signal to send back into the interferometer.

The process of digital sampling is handled by an analog-to-digital converter (ADC) and the process of analog output is handled by a digital-to-analog converter (DAC). Since these converters are linearly mapping a continuous signal onto a discrete range, they are limited by their digital bit depth. For example, a 16 bit ADC is only capable of representing 2^{16} discrete values, or a range from zero to 65536. This range is often centered around zero, giving the ADC the capability to handle a range of ±32768. An incoming analog signal is mapped onto this range and converted into a digital signal.

For example, if I was sampling an analog signal with a range of $\pm100V$, 100V would be mapped to 32768 and -100V would be mapped to -32768 with all of the intermediate voltage values being linearly mapped to the range. This means our digital system would recognize a discrete step size of $100/32768 \approx 3.05mV$.

Looking at the system described above, we must be aware of how our system is going to react when our analog input signal exceeds the intended maximum value of 100V (e.g., a 110V input). The ADC has already assigned its maximum digital value to 100V. This is called range saturation. In this case the ADC will continuously output its maximum value as it has no way to map 110V into a discrete value. The same process can occur in a DAC when a digital signal is sent out at the maximum allowed digital value.

If the digital system is not able to correctly sample and understand an analog error signal, it is easy to imagine a scenario where the reponse of the digital system and the output control signal are not able to complete the control loop as designed. This may cause glitches or misalignments.

We must also consider the fact that many ADCs are calibrated to reflect the intended dynamic range of an optic. If a saturation is occurring, there is a good chance that an optic has moved beyond this intended dynamic range, which also may cause glitches or misalignments.

The ADCs and DACs are monitored by a series of auxiliary channels. The most useful channels are of the form:

```
L1:FEC-21_DAC_OVERFLOW_0_0
```

Parsing this channel name:

```
L1:FEC-{model number}_{ADC/DAC}_OVERFLOW_{ADC/DAC number}_{channel number}
```

These overflow monitor channels are cumulative. If the channel has no saturation at the time of sampling, the overflow channel's reported value will not increase. If the channel was saturated during the last sample, the value of the channel will increase in discrete steps equal in size to the maximum value of the channel.

Discuss Hveto results

Used this to generate flags for veto definer, ETMY driver and OMC DCPD saturations.

2.4 Suspension DAC calibration glitches

We see glitches when suspensions cross values of zero or 2^{16}.

Discuss Hveto results

2.5 RF beatnote whistles

Two RF oscillators beating against one another creates a kHz beatnote that couples into DARM.

2.6 Seismic CPS comb

Oscillators in the capacitive position sensors had drifted apart and caused a beatnote and a comb. Audio analysis pointed towards amplitude modulation.

Fixed by slaving all oscillators to a master.

2.7 DC values of auxiliary channels

No great correlation at the end of the day

2.8   Earthquakes during full lock

Lots of scattering arches during an earthquake, drove up the noise and biased PSD. Caused a sarlacc, removing this data was able to repair data on either side.

2.9   L1 PMC glitches

Characterization of noise and analysis after repair

2.10   Data quality shifts

Performed and mentored data quality shifts.

Chapter 3

IMC Upconversion

3.1 The aLIGO Input Mode Cleaner

LIGO interferometers use several high finesse optical cavities for gravitational wave detection. The lengths of these cavities are controlled using radio frequency (RF) modulation-demodulation techniques in a Pound-Drever-Hall (PDH) locking scheme. This scheme provides a PDH error signal that is linear to cavity length over a specific range. This study examines the specific case of the triangular ring cavity uses in LIGO interferometers for input mode cleaning. When the length of the cavity approaches the boundaries of the PDH error signal linear range, our model of the input mode cleaner PDH response shows that the resulting error signal contains non-linear spectral artifacts. This model and understanding of the non-linear cavity responses will be useful in the commissioning phase of the Advanced LIGO project for more precisely locating and eliminating systematic noise sources in the interfereometers

3.2 Modeling the IMC PDH loop

The PDH response of the cavity was modeled using measured values of optical reflectivity and free spectral range of the Livingston input mode cleaner. The input beam was the nominal LIGO carrier beam with a frequency of $\omega = 281.8$ THz ($\lambda = 1064$ nm) and modulation sidebands of $\Omega = \pm 24$ MHz.

The reflection coefficient of a LIGO input mode cleaner as a function of input beam frequency is given as,

$$F(\omega) = \frac{r(1 + e^{-i\phi})}{1 + r^2 e^{-i\phi}} = \frac{r(1 + e^{-i(\frac{\omega}{\nu_{fsr}})})}{1 + r^2 e^{-i(\frac{\omega}{\nu_{fsr}})}} \tag{3.1}$$

where r is the reflectivity of the input mirror, ϕ is the round-trip phase accumulated when traversing the cavity, and ν_{fsr} is the free spectral range of the cavity [2].

In a situation where the carrier beam is resonant in the cavity and the modulation sidebands are high enough in frequency that they are not resonant, the PDH error signal, here denoted ϵ is given as

$$\epsilon(\omega) = -2\sqrt{P_c P_s} \, \text{Im}\{F(\omega)F^*(\omega + \Omega) - F^*(\omega)F(\omega - \Omega)\}, \tag{3.2}$$

where P_c is the the carrier beam power and P_s is the sideband power [3].

Note: the above error signal is a function of laser frequency. This is an artifact of the original intent of PDH locking: using a fixed length resonant cavity to control the frequency of a laser by forcing it to match the cavity length. We can apply the same technique but flip the direction of feedback and use a highly stable laser to control the length of a free swinging resonant cavity by pushing on the mirrors to match the cavity length to the laser wavelength. The laser frequency detuning and cavity length detuning are linearly mapped to one another using the free spectral range of the resonant cavity.

Importantly, this error signal is linear to the length of the IMC within a certain range of motion. If the optics begin swinging too far away from the nominal locking point, we will begin to see a non-linear response and eventually a lock loss.

To explore this non-linearity, we injected a sinusoidal cavity motion into our model and observed the resulting error signal.

We explored two specific cases. Figure 1 shows spectra of the injected sinusoidal cavity motion (green) and the resulting non-linear error signal (blue). This motion was injected asymetrically about the nominal cavity locking point ($\epsilon = 0$) and therefore we see both even and odd harmonics of the injection frequency.

Figure 2 shows spectra of the injected sinusoidal cavity motion (green) and the resulting non-linear error signal (blue). However, this time the motion was injected symetrically about the nominal cavity locking point and as a result we only see odd harmonics of the fundamental frequency.

We hope to use this model as an explanation of systematic noise found in the aLIGO IMC.

Figure 1 : Sinusoidal cavity motion with frequency 2.78 Hz injected asymmetrically about the locking point of the cavity results in a PDH error signal containing non-linear spectral artifacts at harmonics of the injected cavity motion.
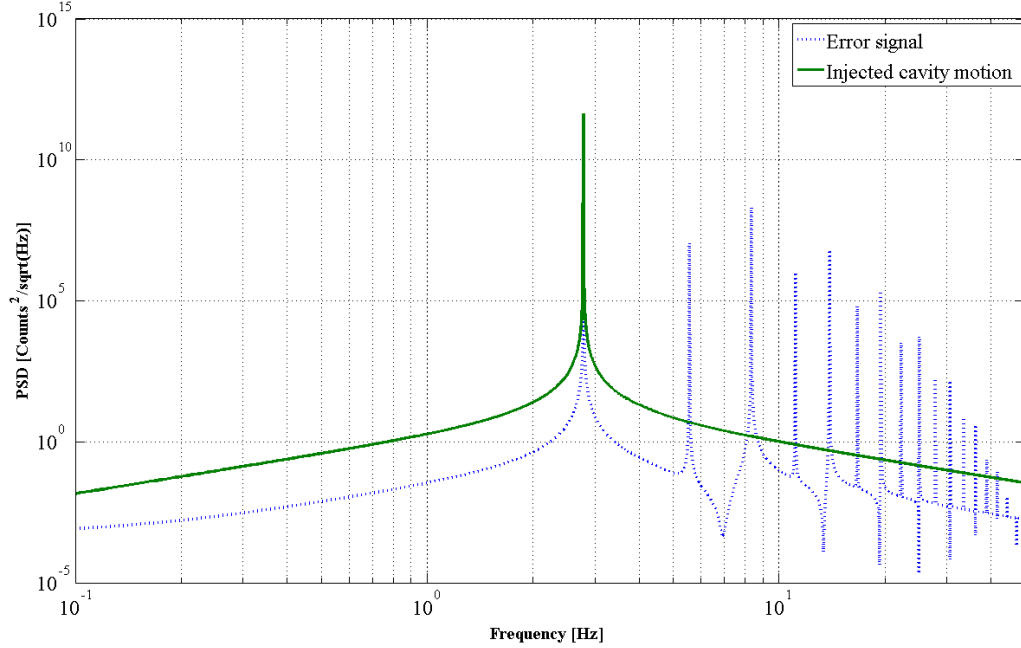
3.3   Upconversion noise in aLIGO

The aLIGO input mode cleaner (IMC) is a triangular ring cavity whose length is sensed and controlled using the PDH locking technique. Each of the three mirrors in the cavity is staged as the bottom mass of a triple suspension in order to passively isolate the mirrors from potential noise sources. In addition, the chambers holding the IMC mirrors are isolated from ground motion by two stages of active seismic isolation. This isolation, however, is not completely impervious to external excitations. During periods of time with excess ground motion we can see seismic noise coupling into the cavity length and its control signal.

Specifically, when we see excess seismic noise in the 1-5 Hz anthropogenic band (believed to be caused by a commercial railroad a few kilometers from the LIGO Livingston Laboratory), we see highly structured noise in the IMC control signal in

Figure 2 : If the motion is symmetric about the cavity locking point, we see only odd harmonics of the injection frequency.
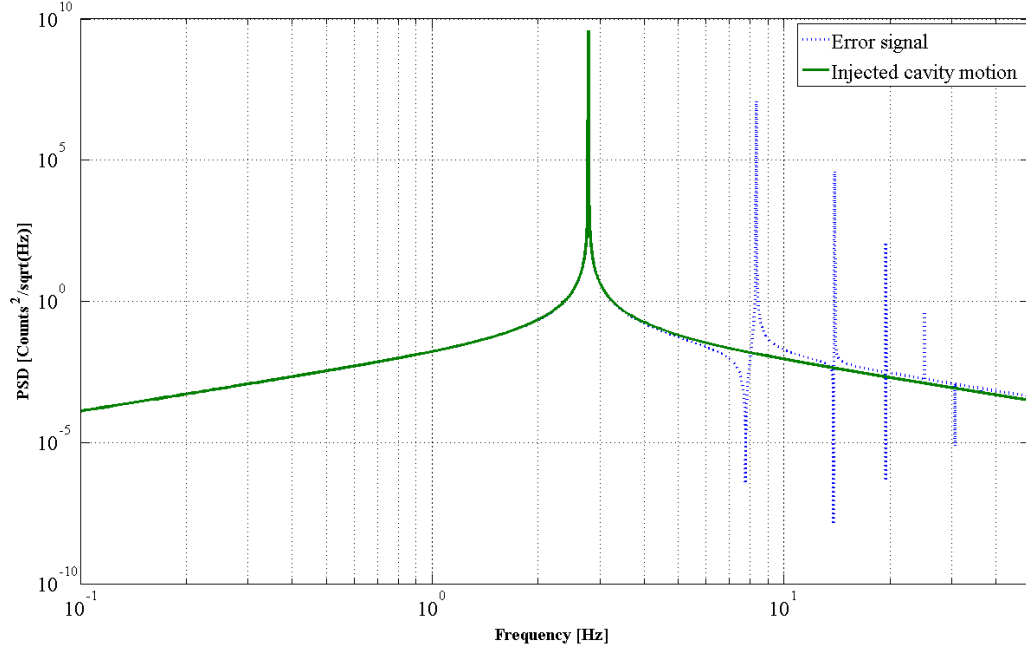
the 10-100 Hz band. This physical mechanism is consistent with the idea of a PDH range saturation. If excess seismic motion reaches the suspension and the optics begin swinging around, it's feasible that they could start to saturate the linear range of the PDH loop.

The noise takes a form very similar in structure to the non-linear PDH signal, displaying strong odd harmonics and weaker even harmonics. The IMC control signal has an associated noise floor that obscures parts of these peaks. The theoretical model uses sinusoids with a highly specified frequency and thus displays very sharp peaks in its spectrum. It should be noted that the peaks in the IMC control signal are the manifestation of a physical process, not digitally generated, and have some natural width to them.

While we have demonstrated that this mechanism is a feasible explanation for the IMC upconversion noise, it has not yet been fully proven. We are currently looking for a better way to look at the actual IMC error point during times of excess seismic motion instead of the control signal.

We also need to localize the source of the 2.78 Hz excitation. Why that specific

Figure 3 : Spectral comb with a fundamental frequncy of 2.78 Hz in the IMC control signal. Red arrows indicate odd harmonics, green arrows indicate even harmonics.
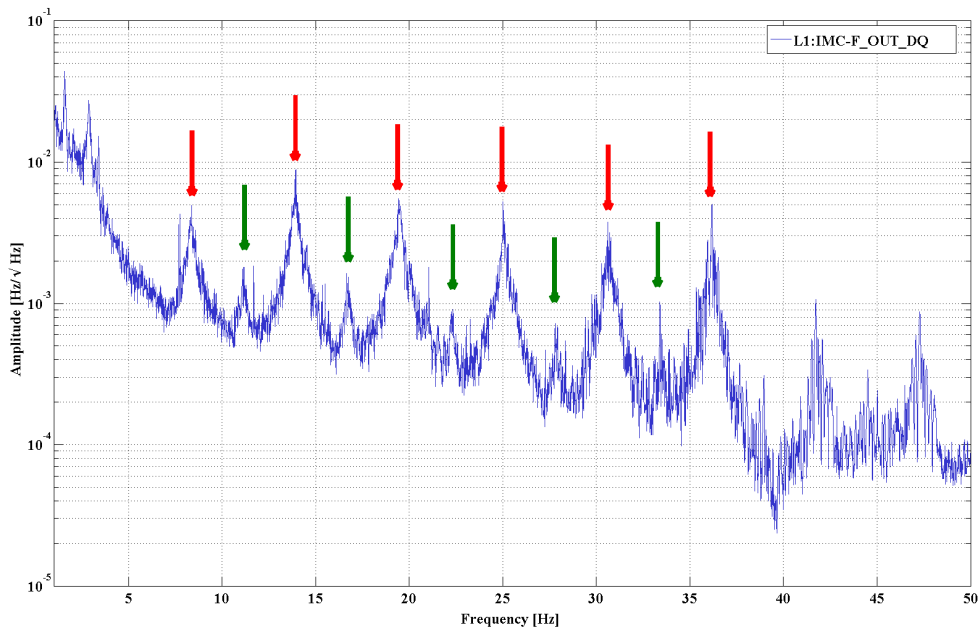
frequency when the excess seismic noise is spread across a 1 - 5 Hz band? We think the source may be a vertical resonance of the triple pendulum suspension that houses the IMC optics being rung up by the excess motion.

We are also going to use the increasing full IFO uptime to figure out whether or not this upconversion noise is coupling downstream into critical cavities such as the recycling or arm cavities.

3.4   Conclusions

We found that injecting sinusoidal cavity motion into our input mode cleaner PDH model generates an error signal with non-linear spectral artifacts, specifically harmonics of the injection frequency, if the cavity motion exceeds the linear PDH range. For cavity motion that is symmetric about the locking point of the error signal, we find that the error signal contains only odd harmonics. For asymmetric cavity motion we find both even and odd harmonics, where the odd harmonics are typically higher in amplitude. In such a case, the amplitude of the even harmonics increases as the

DC offset from the nominal locking point increases, that is, as the cavity motion is more asymmetric.

Chapter 4

Detector Characterization Subsystem Lead

The Online Detector Characterization (ODC) system is an infrastructure designed to extract and record metadata describing the state of the aLIGO interferometers. This state information has two main purposes: to inform data quality investigations by the DetChar group and to serve as a real-time monitor of the interferometer state that can be accessed in the control room. Each subsystem monitored by the DetChar group using an ODC monitor.

The ODC system is unique in that it is runs in real-time in the front-end control system that is used to control the aLIGO interferometers. Each set of ODC monitors is built in Simulink to directly interface with the models that run on the front-end computers. This has several distinct advantages. Since the monitors are run in real-time, they operate in parallel with the control loops that are sensing the various degrees of freedom of the interferometer and are able to achieve highly precise timing. The ODC monitors can also create their own test points, which means an ODC monitor can perform a check on any signal that exists in the front end at its full rate instead of relying on the information that is downsampled and stored in frames. These full rate test points operate at the full sample rate of the model (16384 Hz) and any information recorded in the ODC channel is written at the same rate. In contrast, many channels are only recorded at 16 Hz if they aren't accessed as a test point in the front-end system.

The information generated by each ODC monitor can be extracted and sent to

a segment generation process, where the most useful information is catalogued and represented by segments of time that indicate when a given flag was considered to be active.

4.1 Length Sensing and Control

LSC!

4.1.1 Length locking basics and description of threshold signals

Describe what I did

4.1.2 MEDM screens

Pretty pictures

4.1.3 Summary pages

I made them

4.2 Alignment Sensing and Control

4.2.1 Alignment locking basics and description of threshold signals

Describe what I did

4.2.2 MEDM screens

Pretty pictures!

4.2.3 Summary pages

I made them

4.3 Results

We've been able to use ODC for a few interesting things.

4.3.1 MICH ODC as a witness of RF45 glitches

RF45 glitches cause MICH to wiggle, can flag on this for a veto.

Include VET results for MICH on Omicron triggers.

4.3.2 Using alignment flags as a pre-lockloss flag

Tuned thresholds seem to be decent lockloss predictors.

Measure difference between segment end times and locklosses, histogram values

Chapter 5

Data Quality Vetoes

Description of data quality products

5.1   Why is data quality important?

5.2   Generating data quality flags from instrument channels

5.3   Veto categories

5.4   Veto definer file

Chapter 6

Effects of Data Quality on the PyCBC Background

I did a bunch of CBC DetChar once we had settled the instrument down.

6.1 Data Quality in the PyCBC Pipeline

6.1.1 Gating

6.1.2 χ^2 signal consistency test

6.2 Effects of Data Quality on PyCBC Backgrounds

6.2.1 BNS bin

6.2.2 Bulk bin

6.2.3 Edge bin

6.3 CAT1 vetoes have more impact than CAT2

Chapter 7

Effects of Data Quality on Gravitational Wave Signals

How did data quality impact foreground events?

7.1 GW150914

7.2 GW151226

7.3 G197392

Chapter 8

Limiting Noise Sources in the PyCBC Search

What are the current limiting noise sources?

8.1 Loud transients

8.1.1 Do loud instrumental transients contribute to the newSNR tail?

8.2 Blip glitches

8.2.1 Time-frequency morphology

8.2.2 Time-domain picture with CBC waveforms

8.2.3 What areas of the CBC parameter space are impacted by blips?

8.3 60-200 Hz noise

8.3.1 Time-frequency morphology

8.3.2 What areas of the CBC parameter space are impacted?

Chapter 9

Conclusion

Summarize everything!
Conclude things.

Bibliography

[1] J.A. Sidles and D. Sigg. Optical torques in suspended fabryperot interferometers. *Phys. Lett. A*, 354(3):167 – 172, 2006.

[2] Chris Mueller. The advanced ligo input mode cleaner dcc g1400096.

[3] E. D. Black. An introduction to Pound-Drever-Hall laser frequency stabilization. *Am. J. Phys.*, 69:79–87, 2001.

Curriculum Vitae

Title of Dissertation

 Detector Characterization of Advanced LIGO

Full Name

 Thomas J. Massinger

Place and Date of Birth

 Rochester, NY   July 22, 1989

Colleges and Universities,	Years attended and degrees
Utica College	2007–2011, B.S.
Syracuse University	2011–2016, Ph.D.

Publications

Major Department

 Physics